

XXIst Colloque
GANIL

2019
September 9th – 13th
Strasbourg



**Nuclear structure
of the semi-magic tin isotopes close to ^{100}Sn :
Lifetime measurements of low-lying states in ^{106}Sn and ^{108}Sn**

PhD Thesis Award



INFN
LNL
Istituto Nazionale di Fisica Nucleare

Marco Siciliano

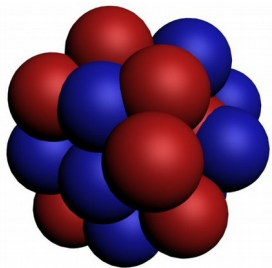


Within the shell model framework, the nuclear interaction can be described via multipole expansion:

$$H = H_0 + \sum H_\lambda$$

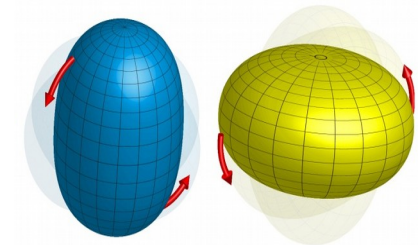
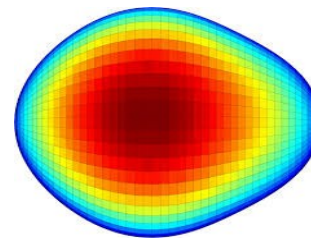
Monopolar Hamiltonian:

- Represent a spherical mean field extracted from the interacting shell model
- Information on the single-particle energies as function of neutron and proton number



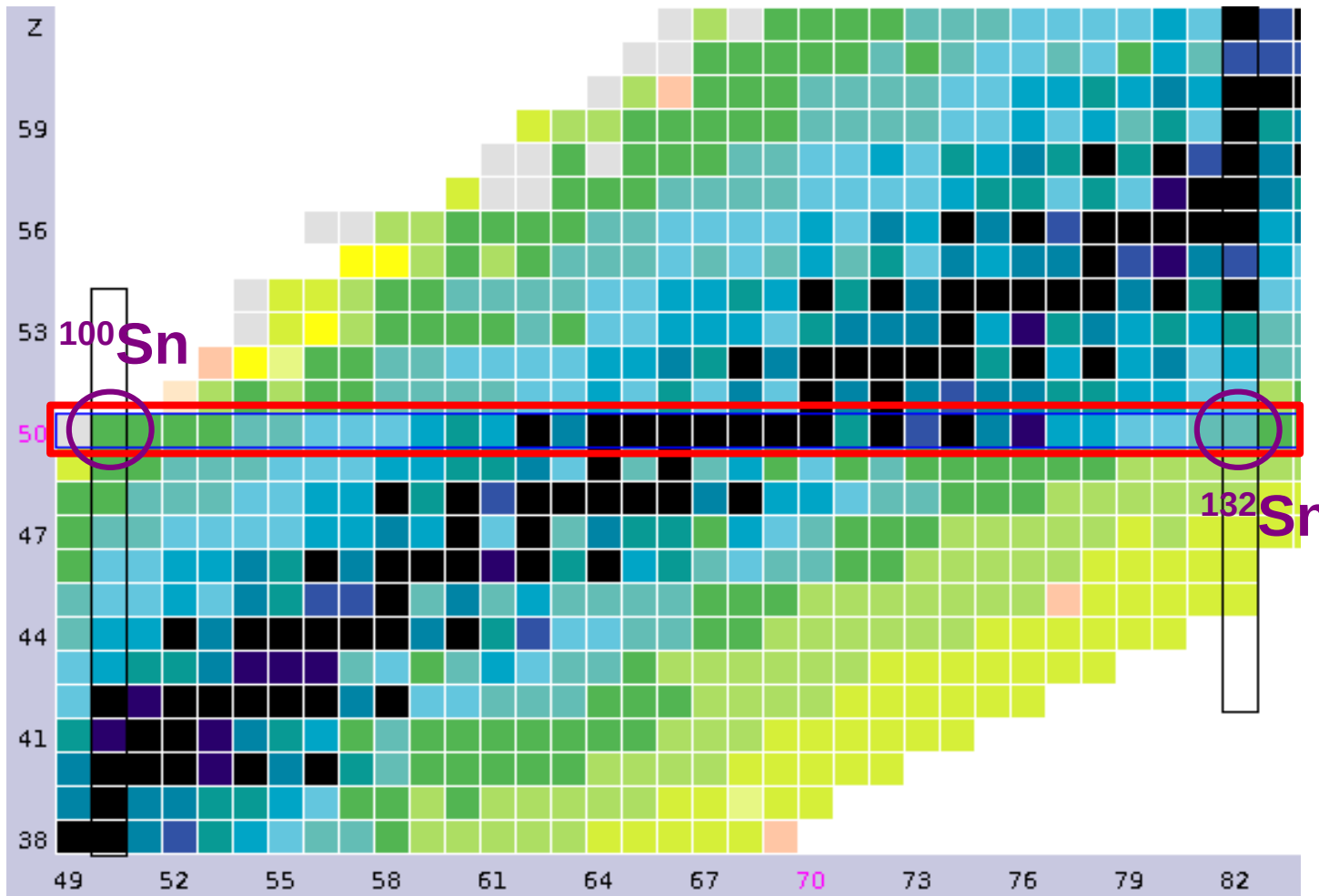
Multipole Hamiltonian:

- Strong correlations between nucleons entails collective motions
- Pairing force drives the nuclear surface to a spherical shape



The balance between the proton-neutron multipole force and the pairing forces determine the nuclear shape and in particular the existence of the **magic numbers**.

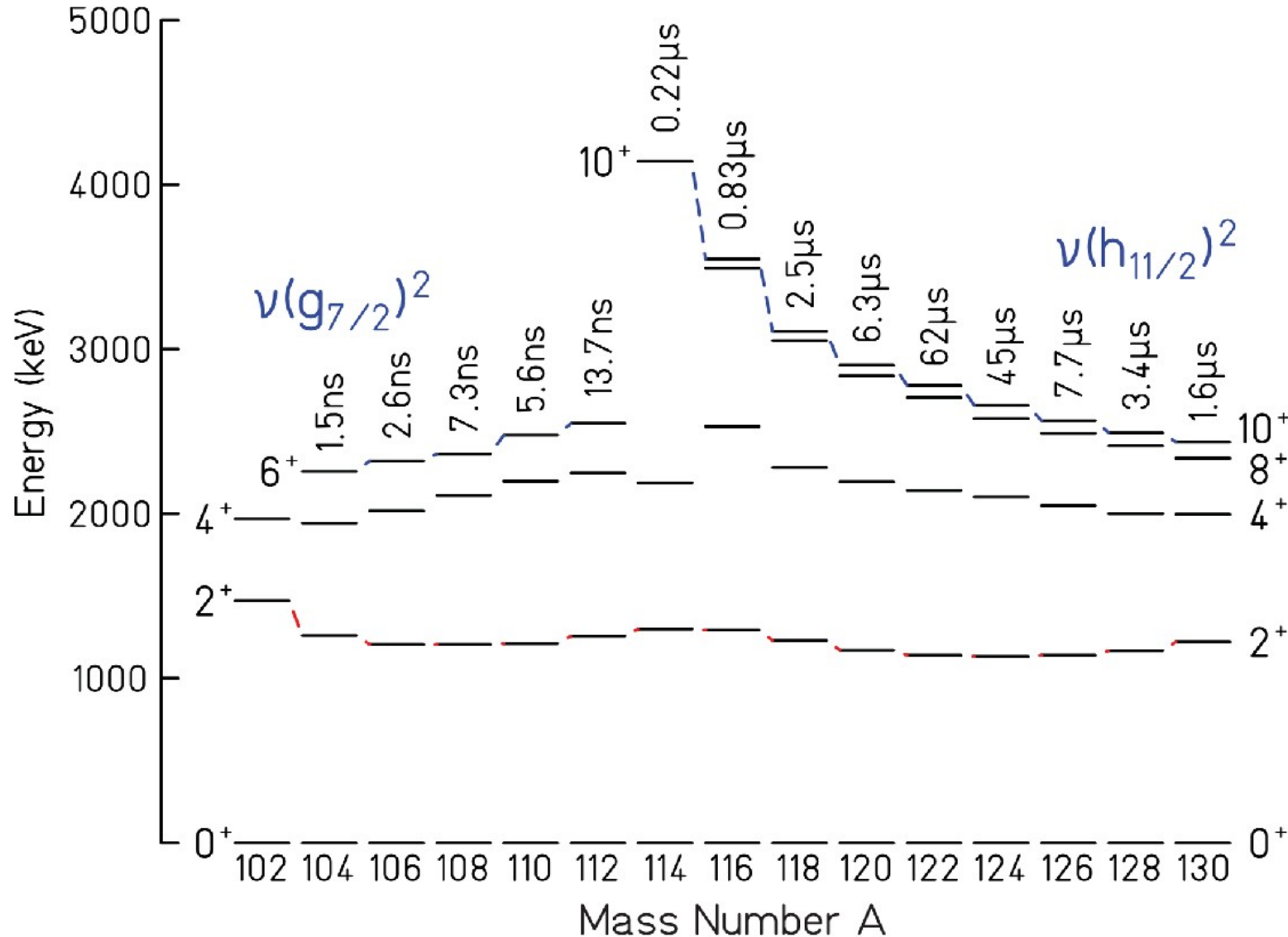
Z=50 PHYSICS CASE



- Longest isotopic chain between two experimentally accessible **doubly-magic nuclei**.
- Unique opportunity for **systematic studies** of the basic nuclear properties.
- Balance between the closed-shell effects and evolving collectivity.

Z=50 PHYSICS CASE

Excitation Energy



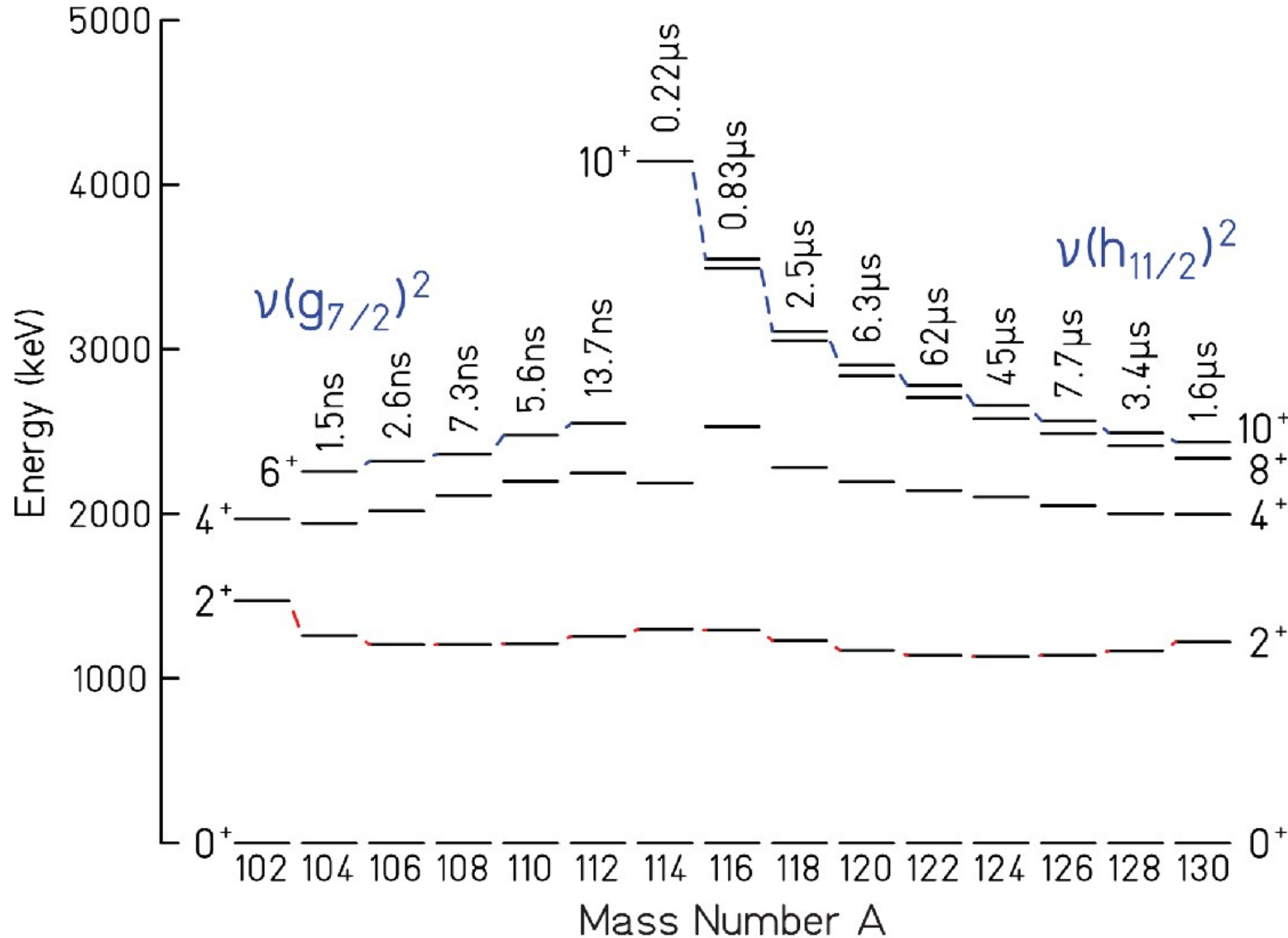
Low-lying isomer

Rather constant excitation energy

R. Kumar et al., Phys. Rev. C 81 (2010) 024306.

Z=50 PHYSICS CASE

Excitation Energy



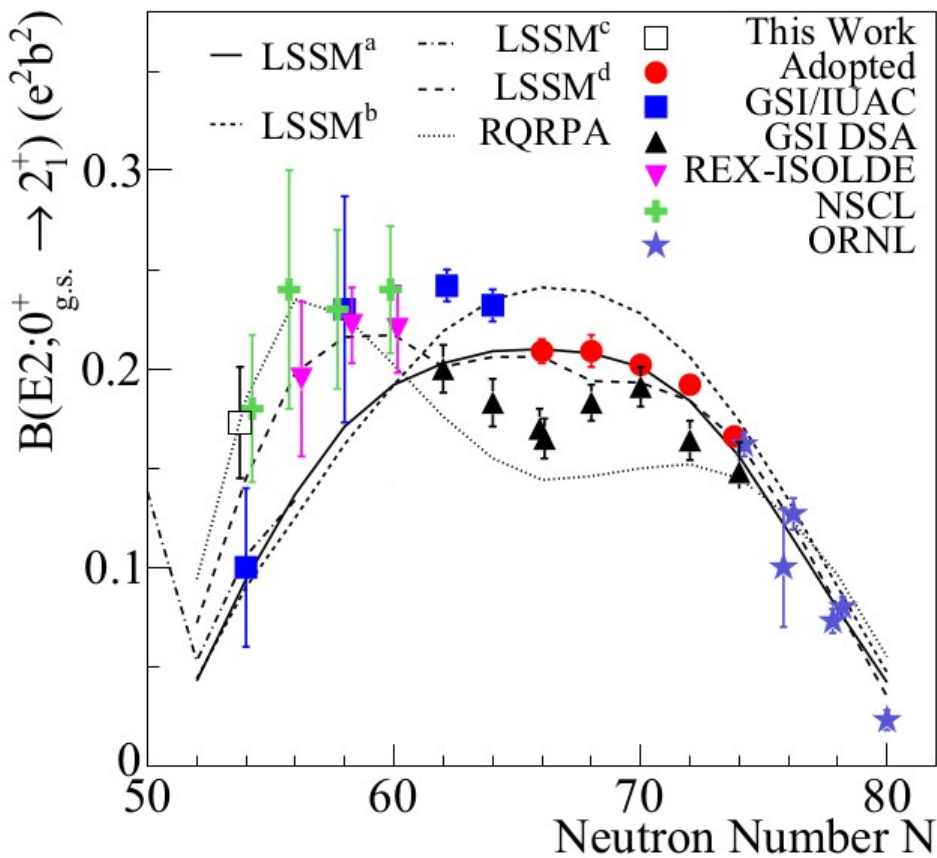
Pairing dominance?

R. Kumar et al., Phys. Rev. C 81 (2010) 024306.

Z=50 PHYSICS CASE

Reduced Transition Probability

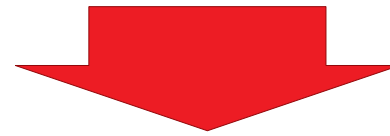
The systematics of the low-lying states excitation energy suggest the **seniority** to be a symmetry of the nuclear Hamiltonian.
Thus, the $B(E2; 2_1^+ \rightarrow 0_{g.s.}^+)$ should present a parabolic behavior with a maximum in the mid-shell.



P. Doornenbal et al., *Phys. Rev. C* 90 (2014) 061302R

For the neutron-deficient nuclei, several experiments have been performed:

- The 6_1^+ isomers limit the investigation of the electromagnetic properties of the low-lying states.
- Coulomb excitation measurements have been performed with radioactive beams, extracting information only on the 2_1^+ states



Multi-nucleon transfer reactions represent a possible solution to overcome the experimental limitations:

- Direct population of the states
- Stable beams

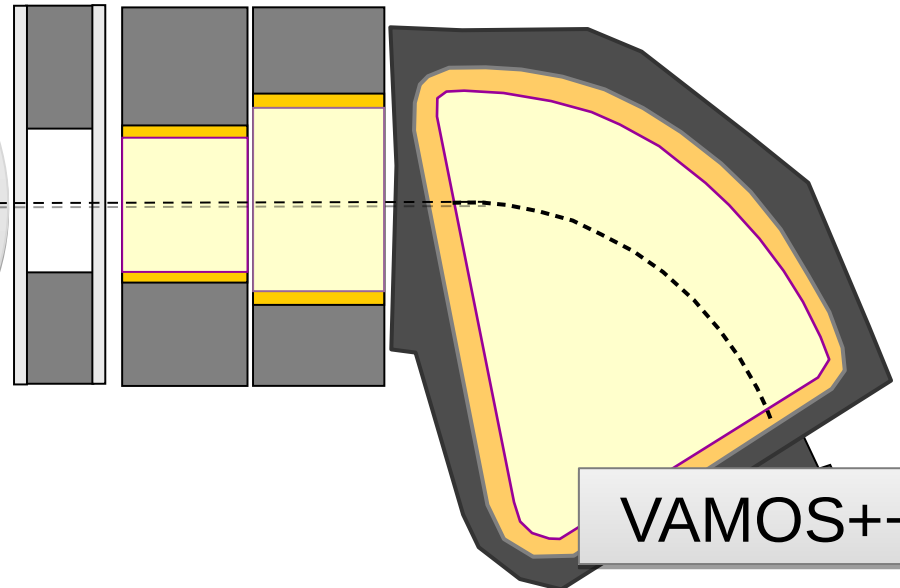
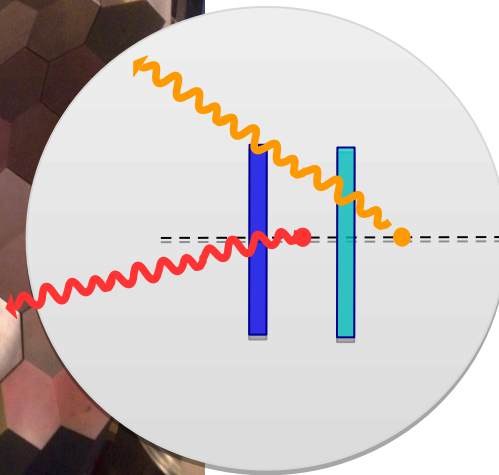
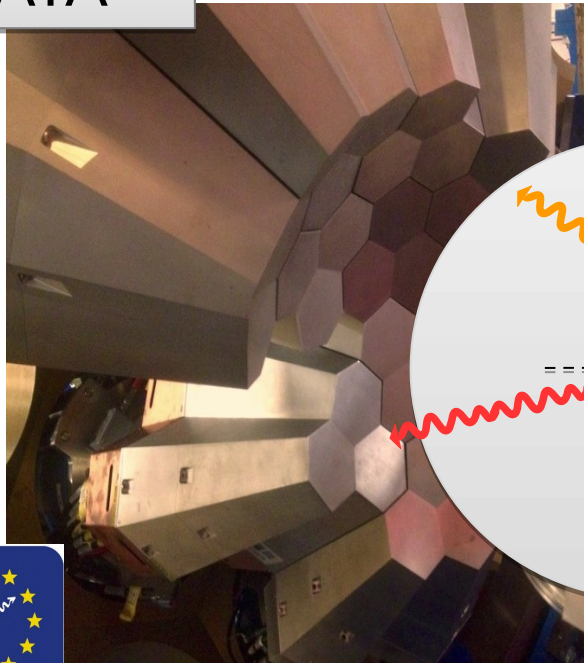
MNT reaction to investigate the neutron-deficient Sn isotopes:

- Stable beam with **higher intensity** than previous experiment with radioactive beams
- **Direct population** of the excited states allows to study also the 4_1^+ states in $^{106,108}\text{Sn}$

Beam: ^{106}Cd @ 770 MeV

Target: ^{92}Mo 0.715 mg/cm²
Degradier: ^{24}Mg 1.6 mg/cm²

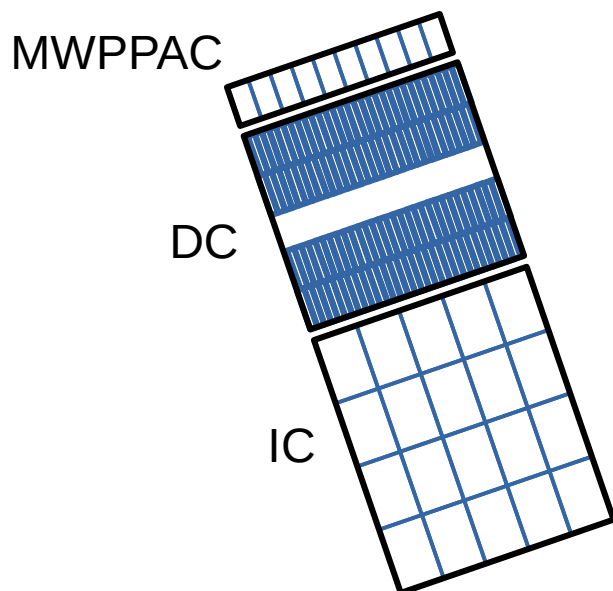
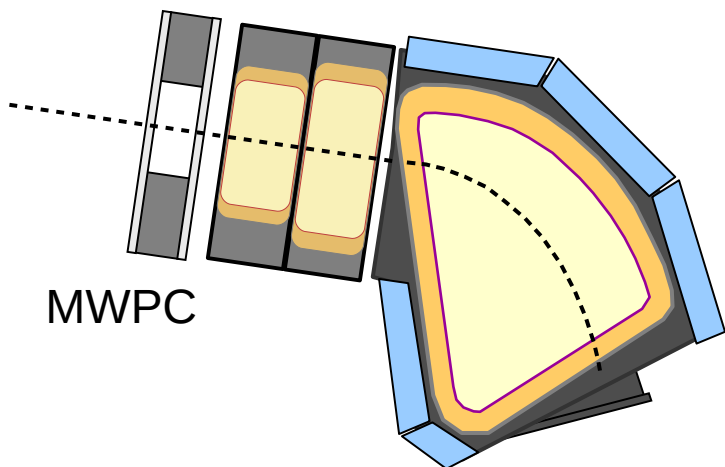
AGATA



VAMOS++

EXPERIMENTAL SETUP

VAMOS++ Spectrometer



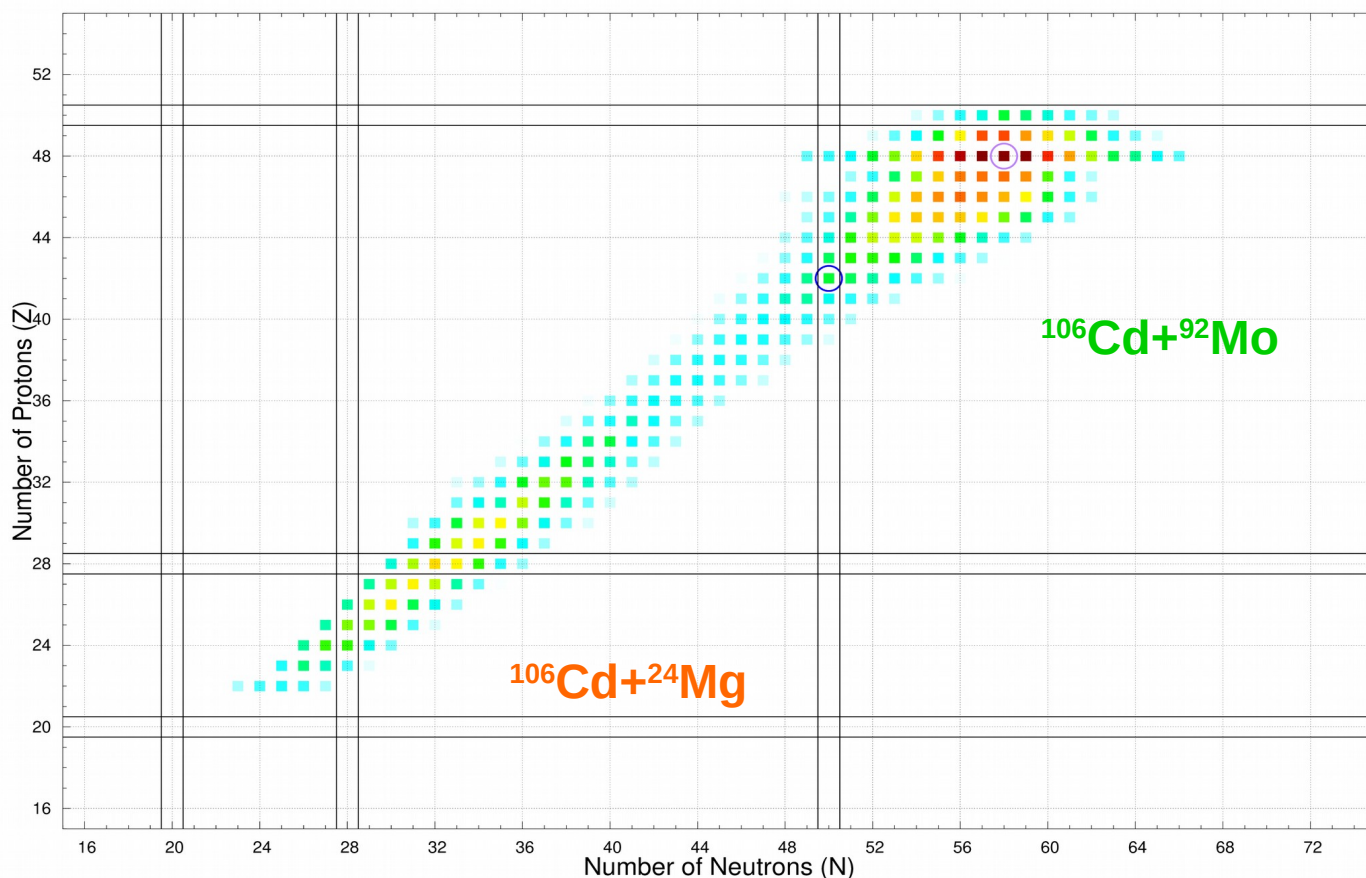
The **V**ARIABLE **M**ODE Spectrometer is a large acceptance magnetic spectrometer used to fully identify the reaction products, providing the atomic number Z and mass A .

- **Optical elements** focalise (2 magnetic quadrupoles) and bend (1 magnetic dipole) the recoil trajectories according to their A/q .
- The dual position sensitive **Multi-Wire Proportional Counter** gives the recoil entrance velocity $\vec{\beta}$, crucial for the Doppler-correction.
- Together with the MWPC, the **Multi-Wire Parallel Plate Avalanche Counter** measures the time-of-flight.
- The **Drift Chambers** provides the fragments direction at the focal-plane position, allowing the trajectory reconstruction.
- The **Ionisation Chamber** measures the reaction products energy loss, providing information about their atomic number (Bethe-Bloch formula).

EXPERIMENTAL SETUP

VAMOS++ Spectrometer

The VAMOS++ spectrometer allows the **complete identification** of the reaction products, providing the atomic number Z and mass A .



From the yield of the identified ions, two region were mainly populated:

- Light ions with $Z \sim 28$ were populated via the fusion-fission reaction of the beam with the degrader material
- Beam-like ions with $Z \sim 48$ were obtained via both multi-nucleon transfer reactions and deep-inelastic collisions of the beam with the target

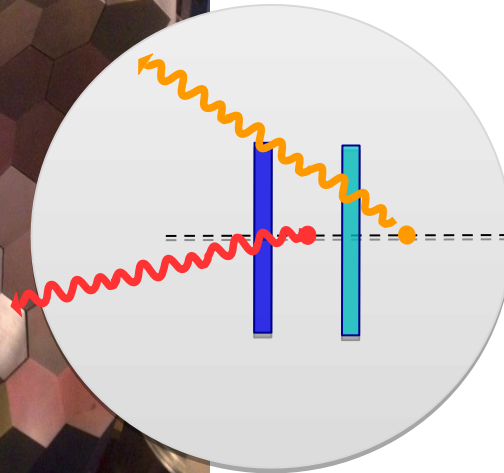
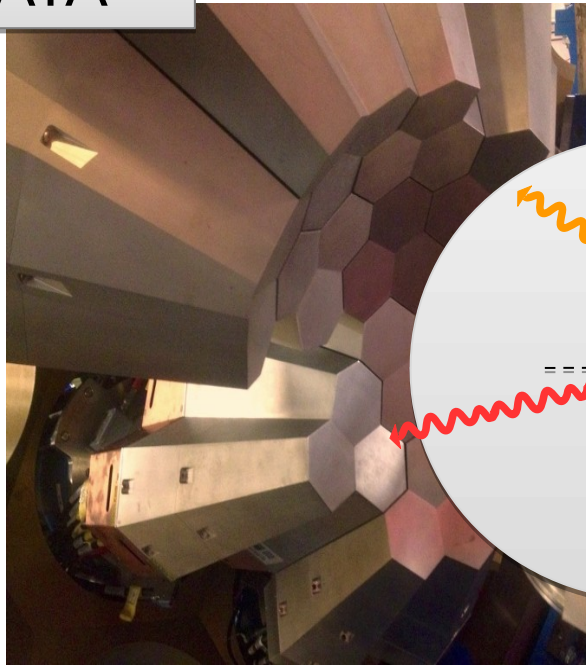
MNT reaction to investigate the neutron-deficient Sn isotopes:

- Stable beam with **higher intensity** than previous experiment with radioactive beams
- **Direct population** of the excited states allows to study also the 4_1^+ states in $^{106,108}\text{Sn}$

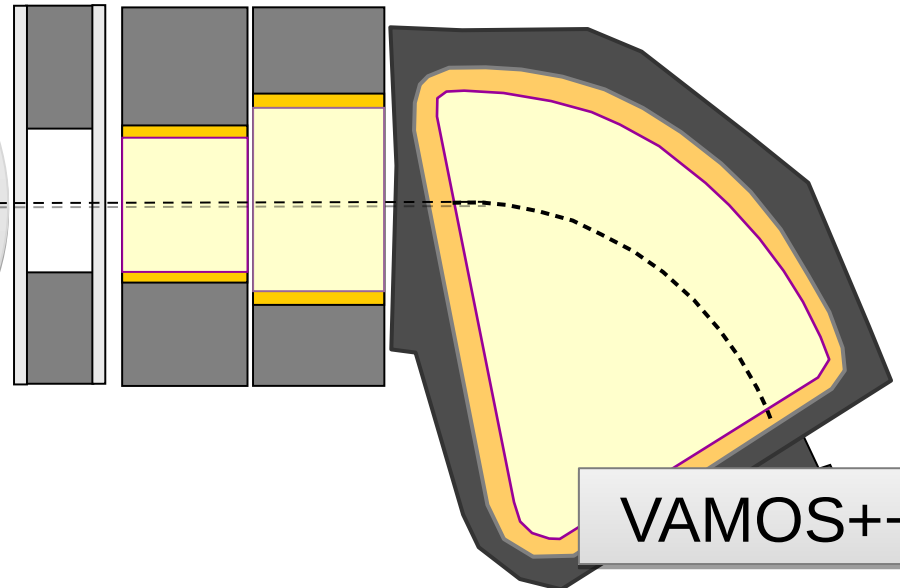
Beam: ^{106}Cd @ 770 MeV

Target: ^{92}Mo 0.715 mg/cm²
Degradator: ^{24}Mg 1.6 mg/cm²

AGATA



GANIL spiral2



VAMOS++

EXPERIMENTAL SETUP

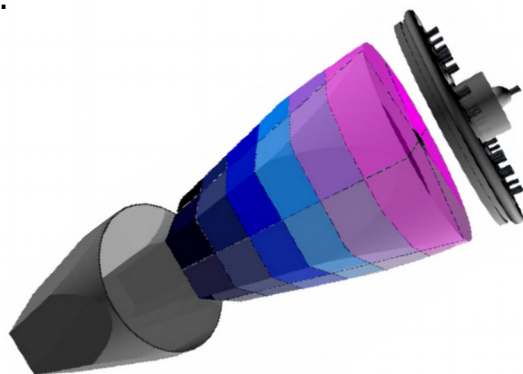
AGATA Spectrometer

Advance **G**amma Tracking Array:

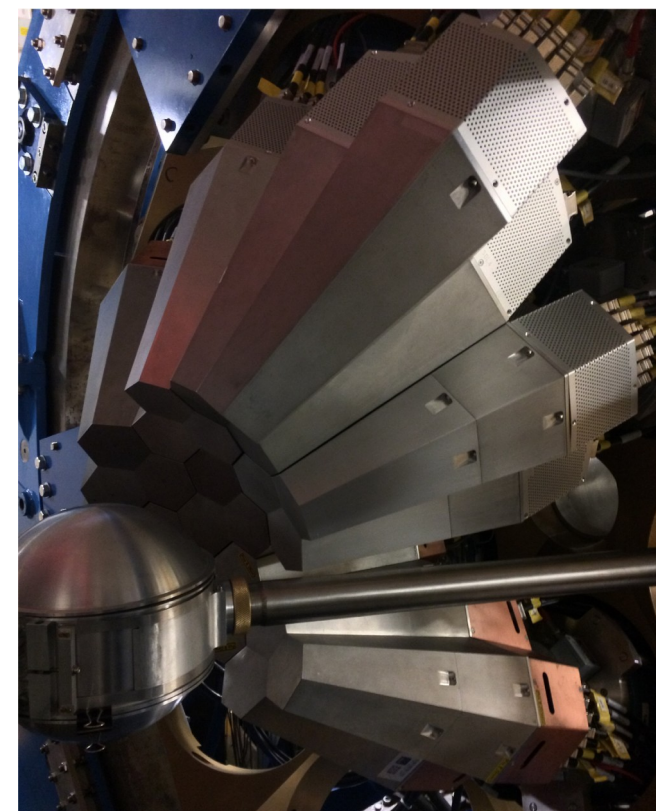
- no anti-Compton shields to increase the active-volume angular coverage and so the **efficiency**
- segmentation of the germanium crystal to improve the **position sensitivity**
- most advance digital electronics allows **high counting rates**



Per each detector 38 signals (36 segments + 2 central contact) are collected together with their traces.



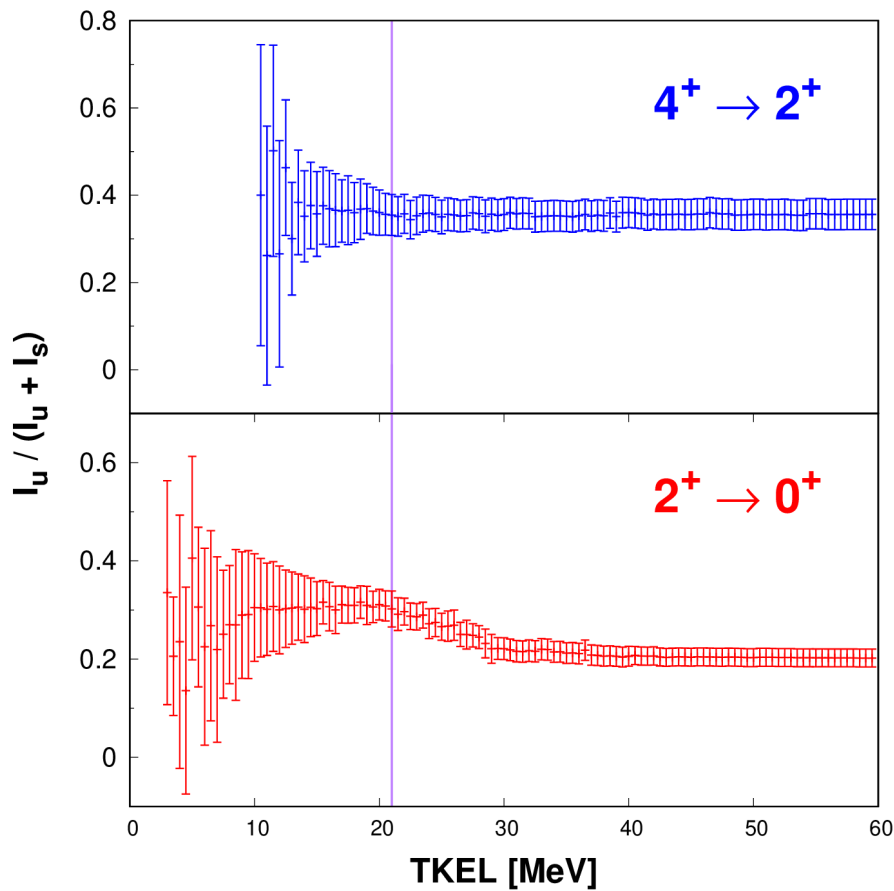
From the comparison between the segments and the central contact signals, various corrections can be applied to **improve or restore the performances** of the apparatus.



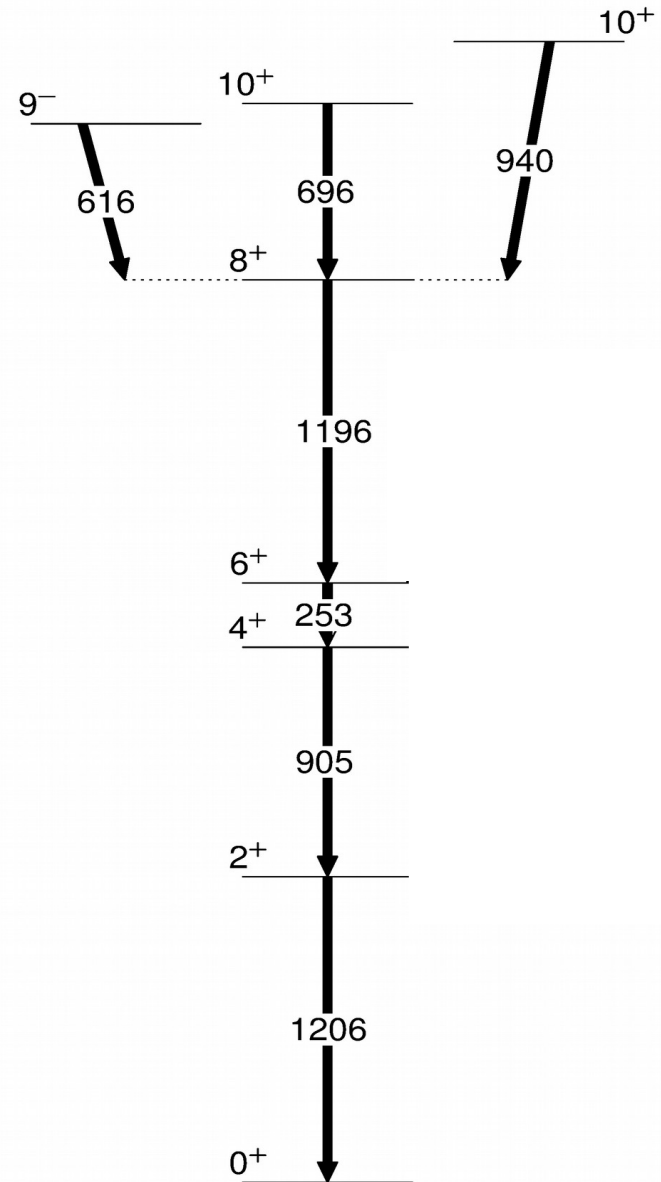
RESULTS

^{108}Sn Lifetimes

The TKEL can be used to **control the direct population** of the excited states and to simplify the decay chain.



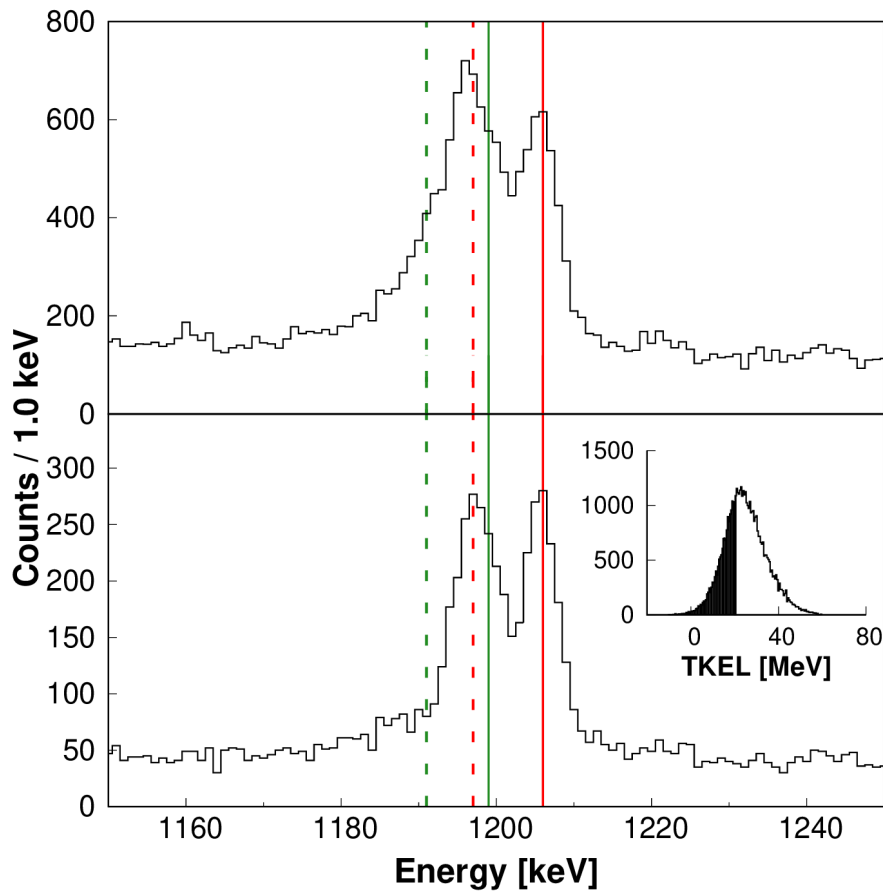
M. Siciliano et al., *Eur. Phys. J.: Conf.* (2019), submitted



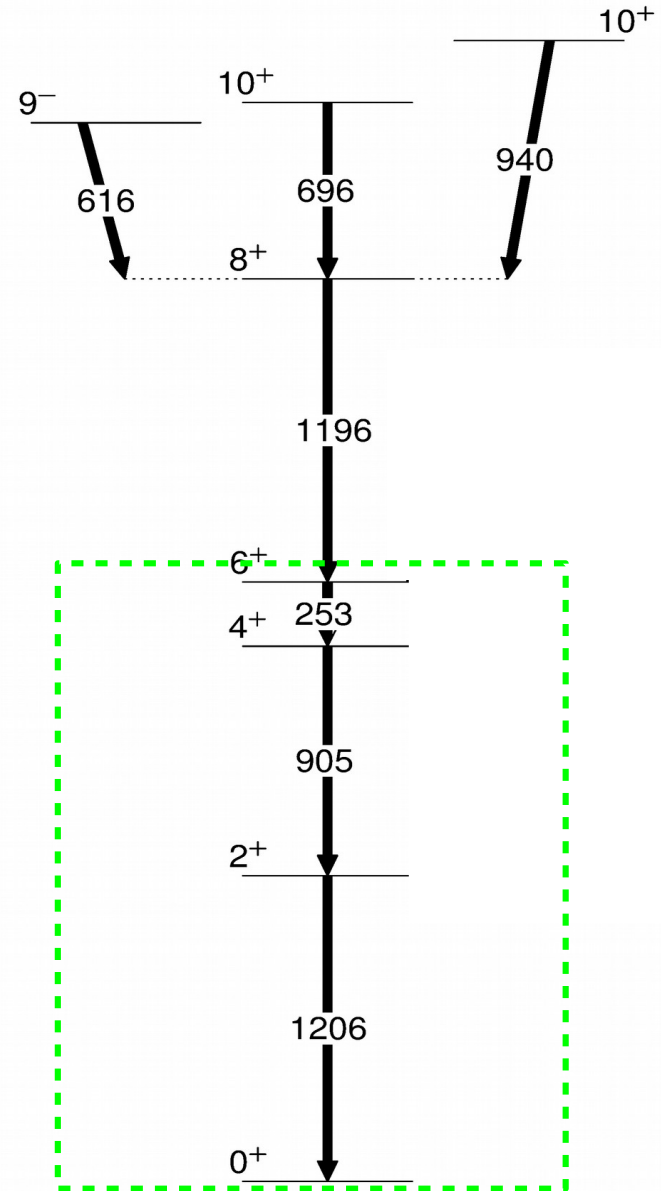
RESULTS

^{108}Sn Lifetimes

The TKEL can be used to **control the direct population** of the excited states and to simplify the decay chain.



M. Siciliano et al., *Eur. Phys. J.: Conf.* (2019), submitted



RESULTS

^{108}Sn Lifetimes

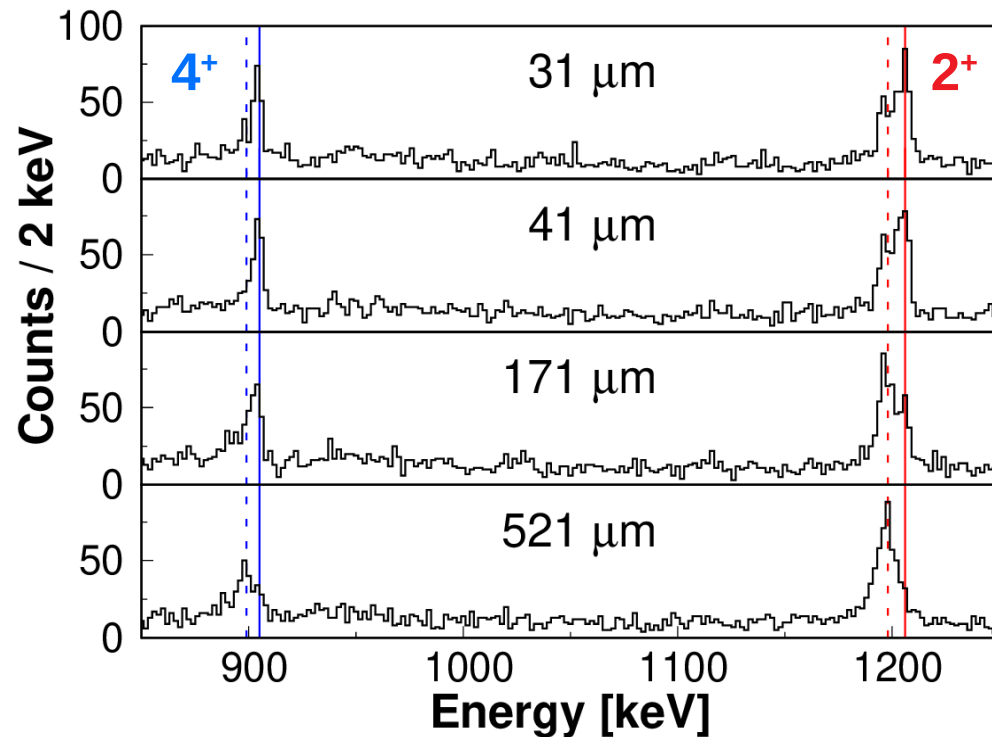
The TKEL can be used to control the **direct population** of the excited states and to simplify the decay chain.

$$\tau(2_1^+) = 0.69(17) \text{ ps}$$

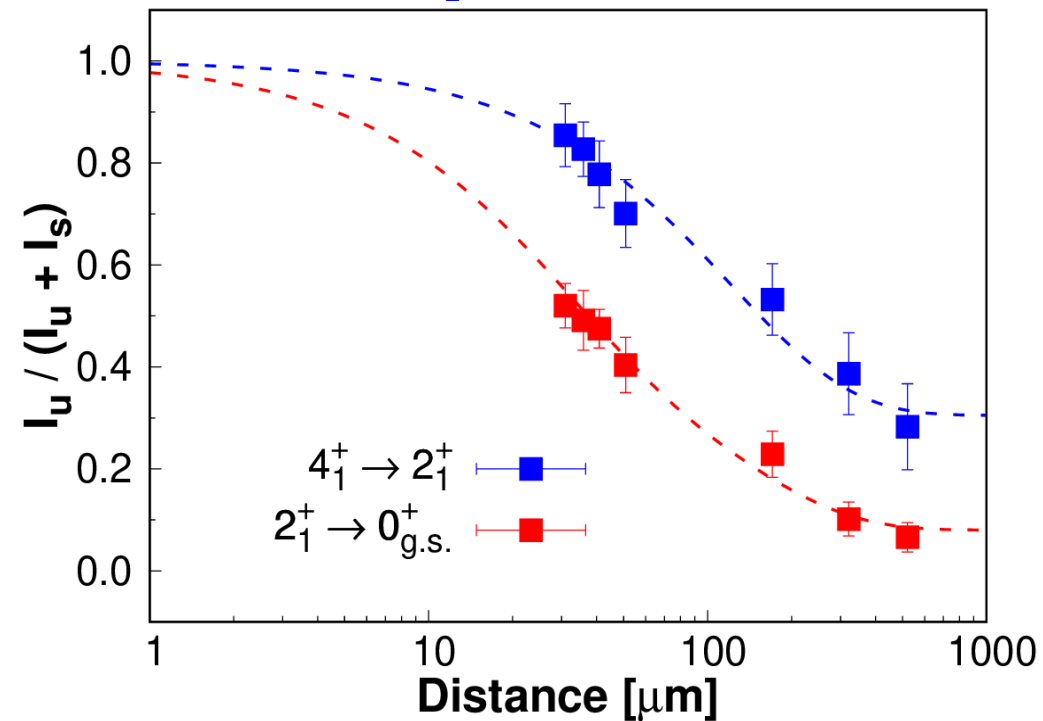
A. Banu et al., Phys. Rev. C 72.(2005) 061305

$$\tau(2_1^+) = 0.76(8) \text{ ps}$$

$$\tau(4_1^+) = 3.6(5) \text{ ps}$$



M. Siciliano et al., Phys. Rev. Lett. (2019), submitted



RESULTS

^{106}Sn Lifetimes

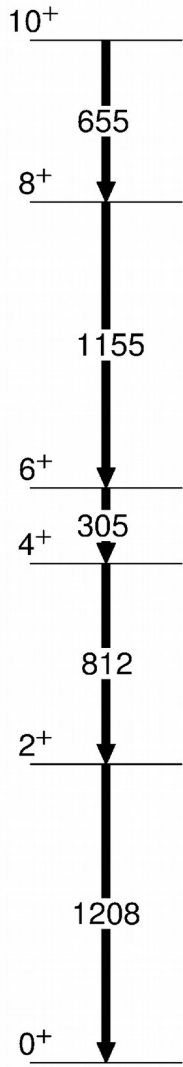
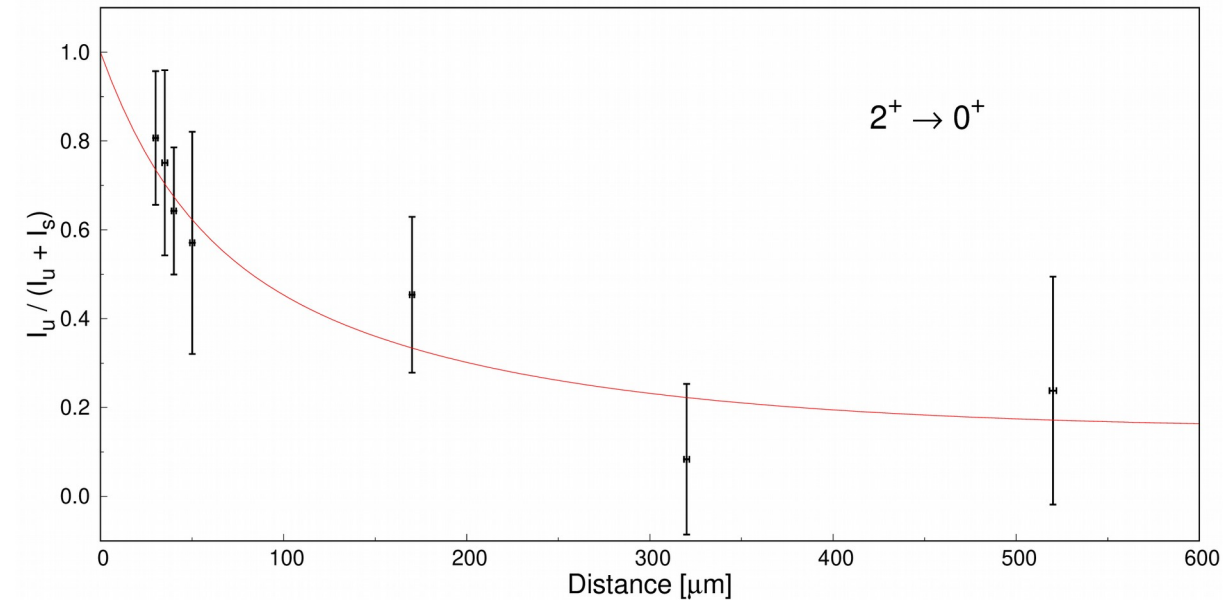
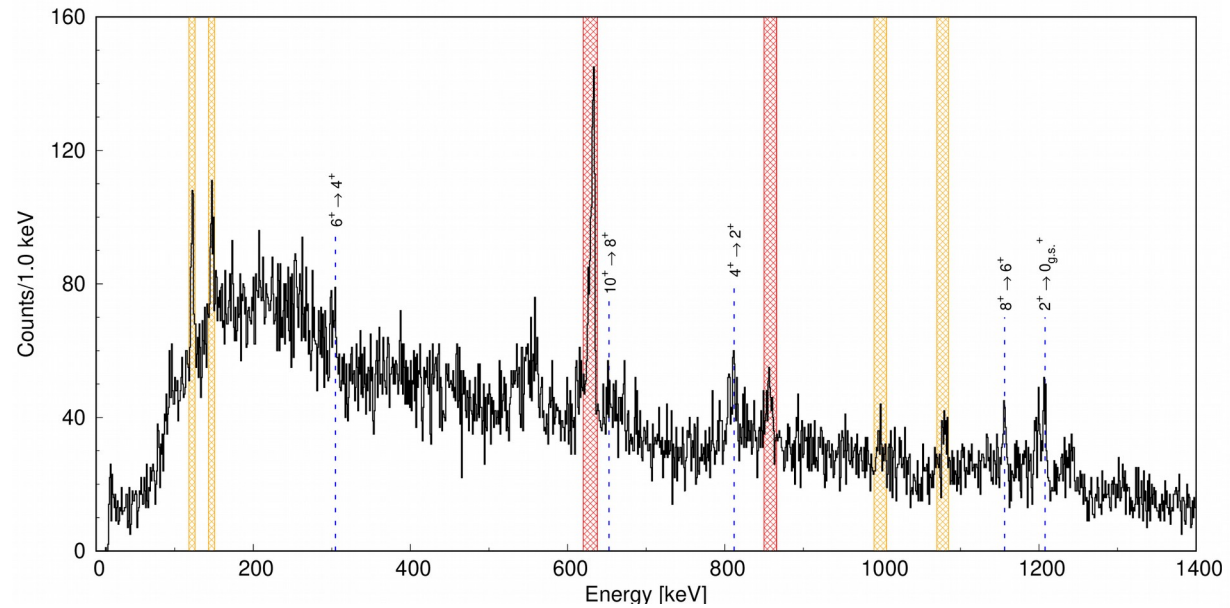
Despite the low cross section of the exotic channel, the neutron-deficient ^{106}Sn was successfully populated and observed.

Contamination from **inelastic-scattered beam** and **In** events does not affect the measurement.

The statistics of ^{106}Sn allow to extract only the decay curve of $2_1^+ \rightarrow 0_{g.s.}^+$ transition.

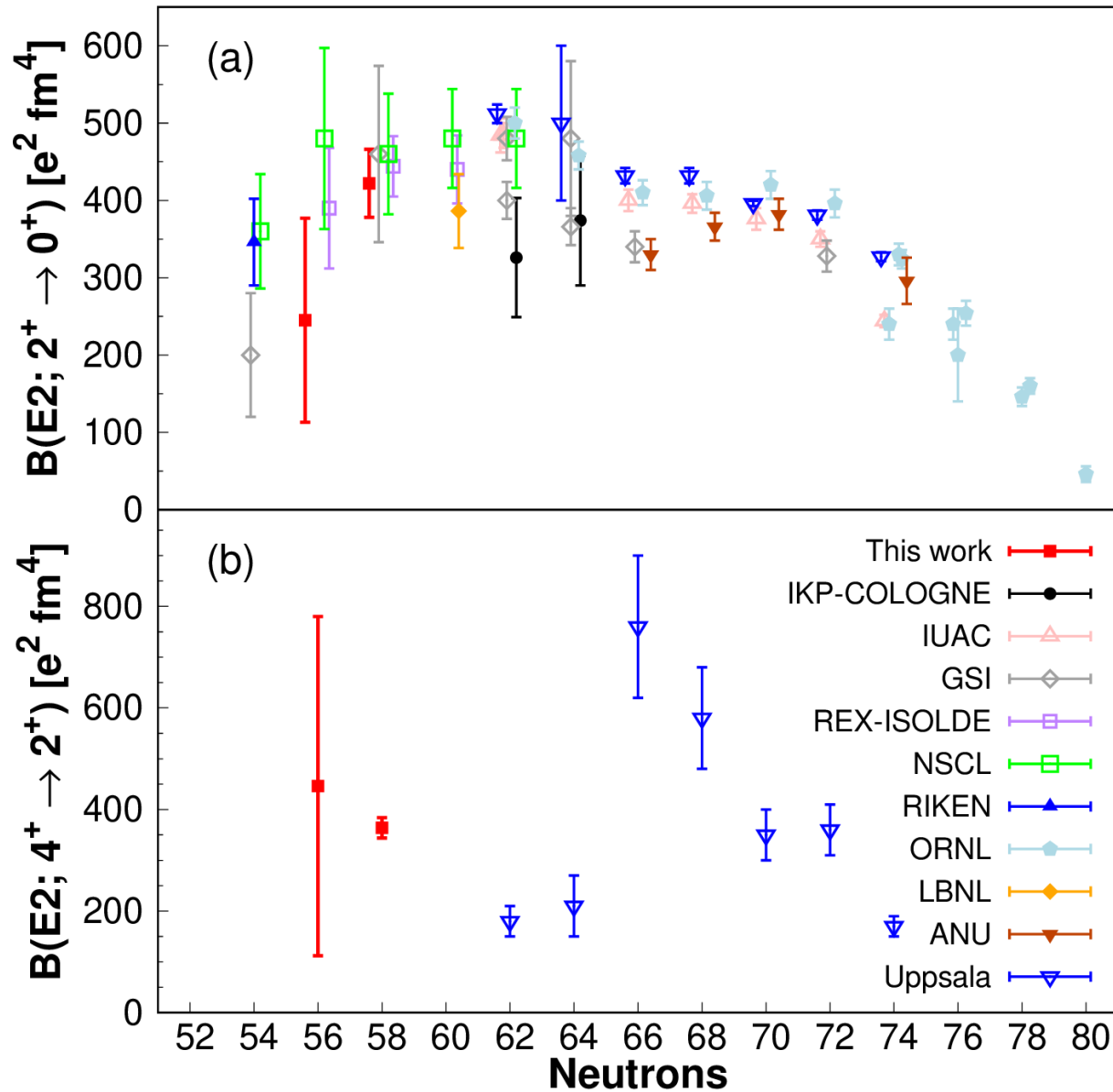
$$\tau(2_1^+) = 1.2(7) \text{ ps}$$

$$\tau(4_1^+) = 5.2(39) \text{ ps}$$



RESULTS

Reduced Transition Probabilities

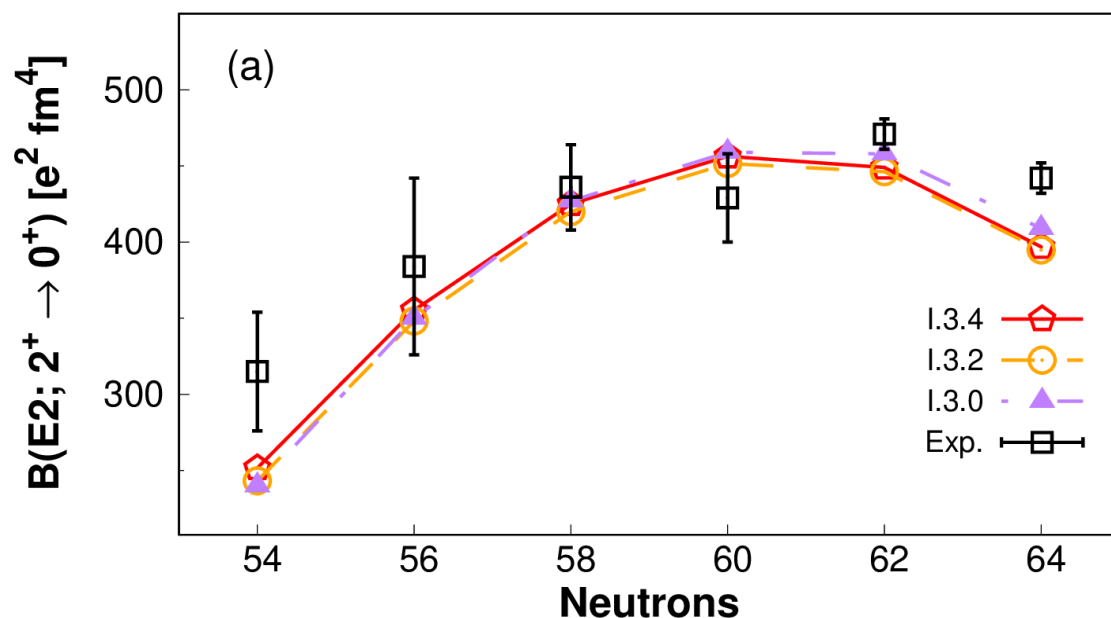


THEORETICAL INTERPRETATION

Quadrupole-Pairing Interplay

Large-scale shell-model calculation, performed by the Strasbourg group, to explain the systematic of the reduced transition probability in the neutron-deficient Sn isotopes.

- Realistic potential: N3LO (CD-Bonn and AV18 provide same results)
- Renormalization: 30% for quadrupole force
0-40% for pairing force
- Monopole-free
 ^{101}Sn single-particle spectrum, given by GEMO
- Full gds valence space
2p-2h excitations in the $(g_{9/2})^\pi$

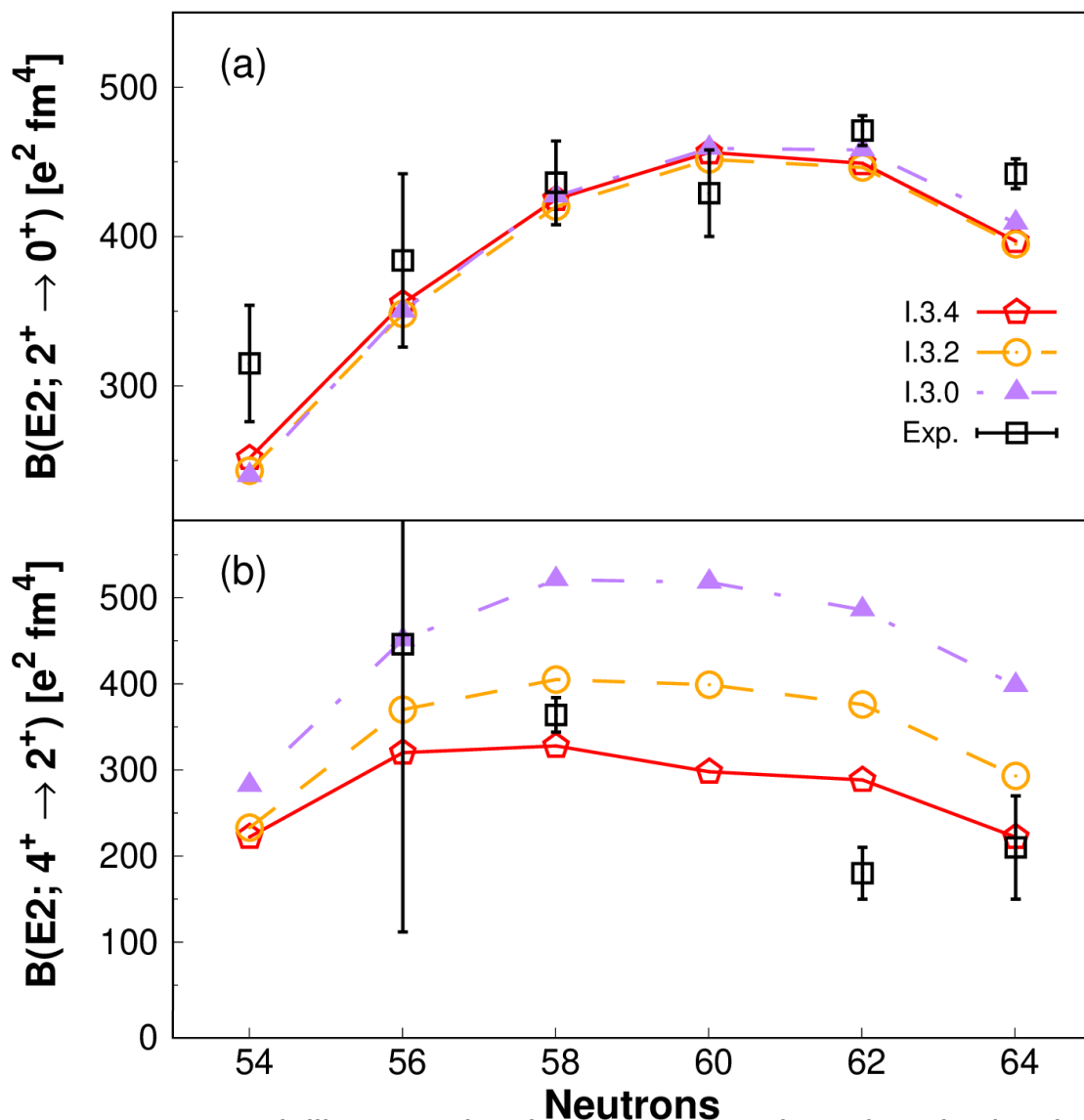


M. Siciliano et al., *Phys. Rev. Lett.* (2019), submitted
A.P. Zuker, *Phys. Rev. Lett.* (2019), accepted

**Quadrupole
dominance**

THEORETICAL INTERPRETATION

Quadrupole-Pairing Interplay



M. Siciliano et al., *Phys. Rev. Lett.* (2019), submitted
A.P. Zuker, *Phys. Rev. Lett.* (2019), accepted

- Realistic potential: N3LO (CD-Bonn and AV18 provide same results)
- Renormalization: 30% for quadrupole force
0-40% for pairing force
- Monopole-free
 ^{101}Sn single-particle spectrum, given by GEMO
- Full gds valence space
2p-2h excitations in the $(g_{9/2})^\pi$

**Pairing force takes its revenge
on quadrupole correlation**

**Results in ^{108}Sn allow to firmly
define the pairing force**

- Deep-inelastic collisions are a powerful tool for populating the region close to ^{100}Sn . Thanks to the direct population of the states, electromagnetic properties of the low-lying states can be investigated.
- For the very first time **the lifetime of the 2_1^+ and 4_1^+ states has been measured for $^{106-108}\text{Sn}$.**
- The extracted $B(E2)$ values have been compared with LSSM calculations to explain the trend of neutron-deficient Sn isotopes.
 - Despite quadrupole force is reduced to its realistic value, the **$B(E2; 2_1^+ \rightarrow 0_{g.s.}^+)$ values are not affected by pairing** renormalization. Quadrupole correlations dominate.
 - The **$B(E2; 4_1^+ \rightarrow 2_1^+)$ values are sensitive** to the form of the nuclear interaction. The precise results in ^{108}Sn allow to firmly define the amount of pairing renormalization

The very precise measurements in ^{108}Sn have shown to open new perspectives in the understanding of the quadrupole-pairing interplay.

THANKS FOR YOUR ATTENTION...

M. Siciliano^{1,2,3}, J.J. Valiente-Dobón¹, A. Goasduff^{1,2,4}, F. Nowacki⁵, A.P. Zuker⁵,
D. Bazzacco⁴, A. Lopez-Martens⁶, E. Clément⁷, G. Benzoni⁸, T. Braunroth⁹, N. Cieplicka-Oryńczak^{8,10}, F.C.L. Crespi^{8,11},
G. de France⁷, M. Doncel¹², S. Ertürk¹³, C. Fransen⁹, A. Gadea¹⁴, G. Georgiev⁶, A. Goldkuhle⁹, U. Jakobsson¹⁵,
G. Jaworski^{1,16}, P.R. John^{2,4,17}, I. Kuti¹⁸, A. Lemasson⁷, H. Li¹⁵, T. Marchi¹, D. Mengoni^{2,4}, C. Michelagnoli^{7,19}, T. Mijatović²⁰,
C. Müller-Gatermann⁹, D.R. Napoli¹, J. Nyberg²¹, M. Palacz¹⁶, R.M. Pérez-Vidal¹⁴, B. Sayđi^{1,22}, D. Sohler¹⁸, S. Szilner²⁰,
D. Testov^{2,4}, D. Barrientos²³, B. Birkenbach⁹, H.C. Boston²⁴, A.J. Boston²⁴, B. Cederwall²⁵, D.M. Cullen²⁶, J. Collado²⁷,
P. Désesquelles⁶, J. Dudouet^{6,28}, C. Domingo-Pardo¹⁴, J. Eberth⁹, F.J. Egea-Canet¹, V. González²⁷, D.S. Judson²⁴,
L.J. Harkness-Brennan²⁴, H. Hess⁹, A. Jungclaus²⁹, W. Korten³, M. Labiche³⁰, A. Lefevre⁷, S. Leoni^{8,11}, A. Maj¹⁰,
R. Menegazzo⁴, B. Million⁸, A. Pullia^{8,11}, F. Recchia^{2,4}, P. Reiter⁹, M.D. Salsac³, E. Sanchis²⁷, O. Stezowski²⁸,
Ch. Theisen³, and M. Zielińska³

¹ INFN, Laboratori Nazionali di Legnaro, Italy.

² Dipartimento di Fisica e Astronomia, Università di Padova, Italy.

³ Irfu/CEA, Université de Paris-Saclay, Gif-sur-Yvette, France.

⁴ INFN, Sezione di Padova, Italy.

⁵ IPHC, CNRS/IN2P3 Université de Strasbourg, France.

⁶ CSNSM, CNRS/IN2P3, Université de Paris-Saclay, Orsay, France.

⁷ GANIL, Irfu/CEA/DRF and CNRS/IN2P3, Caen, France.

⁸ INFN, Sezione di Milano, Italy.

⁹ IKP, Universität zu Köln, Germany.

¹⁰ IFJ-PAN, Krakow, Poland.

¹¹ Dipartimento di Fisica, Università di Milano, Italy.

¹² Universidad de Salamanca, Salamanca, Spain.

¹³ Ömer Halisdemir Üniversitesi, Niğde, Turkey.

¹⁴ IFIC, CSIC-Universidad de Valencia, Spain.

¹⁵ Kungliga Tekniska Högskolan, Stockholm, Sweden.

¹⁶ HIL, University of Warsaw, Poland.

¹⁷ IKP, Technische Universität Darmstadt, Darmstadt, Germany.

¹⁸ INR, Hungarian Academy of Sciences, Debrecen, Hungary.

¹⁹ Institut Laue-Langevin, Grenoble, France.

²⁰ Ruder Bošković Institute and University of Zagreb, Croatia.

²¹ Institutionen för Fysik och Astronomi, University of Uppsala, Sweden.

²² Ege Üniversitesi, İzmir, Turkey.

²³ CERN, Geneva, Switzerland.

²⁴ Oliver Lodge Laboratory, University of Liverpool, UK.

²⁵ Department of Physics, Royal Institute of Technology, Stockholm, Sweden.

²⁶ Schuster Laboratory, University of Manchester, UK.

²⁷ Departamento de Ingeniería Electrónica, Universidad de Valencia, Spain.

²⁸ IPN-Lyon, CNRS/IN2P3, Université de Lyon, Villeurbanne, France.

²⁹ Instituto de Estructura de la Materia, CSIC, Madrid, Spain.

³⁰ STFC Daresbury Laboratory, Warrington, UK.